

Article

Synthesis, Structural, Thermal, and Hirshfeld Surface Analysis of In(III) Tris (*N*-Methyl-*N*-Phenyl Dithiocarbamate)

Hela Ferjani ¹  and Damian C. Onwudiwe ^{2,3,*} 

¹ Chemistry Department, College of Science, Imam Mohammad Ibn Saud Islamic University (IMSIU), Riyadh 11623, Saudi Arabia

² Materials Science Innovation and Modelling (MaSIM) Research Focus Area, Faculty of Natural and Agricultural Science, North-West University (Mafikeng Campus), Private Bag X2046, Mmabatho 2735, South Africa

³ Department of Chemistry, Faculty of Natural and Agricultural, Science, North-West University (Mafikeng Campus), Private Bag X2046, Mmabatho 2735, South Africa

* Correspondence: damian.onwudiwe@nwu.ac.za

Abstract: The reaction of ammonium *N*-methyl-*N*-phenyl dithiocarbamate with In³⁺ resulted in the In(III) tris (*N*-methyl-*N*-phenyl dithiocarbamate) complex. The spectroscopic characterization of the complex was carried out using FTIR, ¹H, and ¹³C NMR spectroscopy. Single-crystal X-ray diffraction analysis (SCXRD) revealed that the complex crystallizes in a triclinic system with a centrosymmetric P-1 space group. The stabilization of the structure was via weak hydrogen bonds and C-H···π contacts. The non-covalent interactions in the crystal network were identified using computational analysis based on SCXRD data, such as Hirshfeld surface analysis. The thermal decomposition behaviour of the complex was studied by thermogravimetric analysis, which showed a one-step decomposition to yield In₂S₃ at 380 °C.

Keywords: indium complex; crystal structure; dithiocarbamates; Hirshfeld surface analysis; thermogravimetry



Citation: Ferjani, H.; Onwudiwe, D.C. Synthesis, Structural, Thermal, and Hirshfeld Surface Analysis of In(III) Tris (*N*-Methyl-*N*-Phenyl Dithiocarbamate). *Inorganics* **2022**, *10*, 146. <https://doi.org/10.3390/inorganics10100146>

Academic Editor: Duncan H. Gregory

Received: 18 August 2022

Accepted: 16 September 2022

Published: 20 September 2022

Publisher's Note: MDPI stays neutral with regard to jurisdictional claims in published maps and institutional affiliations.



Copyright: © 2022 by the authors. Licensee MDPI, Basel, Switzerland. This article is an open access article distributed under the terms and conditions of the Creative Commons Attribution (CC BY) license (<https://creativecommons.org/licenses/by/4.0/>).

1. Introduction

The chemistry of the main group and transition metal compounds obtained from dithiocarbamates ligands has been widely explored in the past four decades [1,2]. The sustained interest in these compounds could be ascribed to their diverse applications in medicine [3,4], agriculture [5], industry [6], and in catalysis [7,8]. In addition to their wide applications, these compounds show great structural diversity. Their tendency to exhibit a different remarkable range of structures has been attributed to the ability of dithiocarbamate to display different coordination modes including monodentate, isobidentate, anisobidentate, and triconnective [9]. The compounds generally adopt an associated structure that is created via secondary intermolecular M···S interactions, resulting in polymeric supramolecular assemblies [10], although discrete monomeric structures also exist [11].

Dithiocarbamate complexes of main group elements are relatively less studied compared to the transition elements [12]. Among the main group elements, the dithiocarbamate complexes of Group 13 elements are one of the most interesting compounds due to their structural chemistry and application as molecular precursors for the synthesis of M₂S₃ nanoparticles [13]. For example, the chemistry of Ga and In dithiocarbamate complexes using internally functionalized dithiocarbamates has been reported. Structurally, indium dithiocarbamate is monomeric with three dithiocarbamate groups chelated to the indium atom. The literature shows sparse reports on indium(III) tris (dithiocarbamate) complexes, and this paper reports the synthesis and characterization of the indium(III) complex with *N*-methyl-*N*-phenyl dithiocarbamate. The complexes have been characterized by FTIR, NMR spectroscopy, thermal and Hirshfeld surface analysis techniques.

2. Results and Discussion

2.1. Spectroscopic Analysis

In the FTIR spectrum, the formation of the complex was identified through the presence of certain vibrational frequencies, primarily the $\nu\text{C-N}$ (thioureide) and $\nu\text{C-S}$ stretching vibrations at 1502 and 977 cm^{-1} , respectively. While the peak position of the former gives an indication of the contribution by the partial double-bond of the polar ($\text{C}=\text{N}^+$) structure of thioureide, that of the latter signifies the coordination format (bidentate/monodentate) of dithiocarbamate ligands [14]. The behaviour of the $\nu\text{C-N}$ (thioureide) has been ascribed to its double bond character created by the flow of electron via the electron-releasing tendency of the amines. This electron flow is responsible for the high density of electrons towards the sulphur atoms through the thioureide π -system, thereby resulting in a shift of the vibrational frequency to a region of higher energy [14,15]. The $\nu\text{C-S}$ stretching bands around 977 cm^{-1} appeared as a single band with no splitting, which indicated a bidentate mode of coordination of the dithiocarbamate ligand to the indium atom [16].

The ^1H NMR spectrum of the complex (Figure 1a) showed a singlet signal around 3.70 ppm associated with the methyl group bound to the nitrogen of the dithiocarbamate. A high deshielding of the protons is observed, which was due to the closeness of the atoms to the thioureide nitrogen compared to the free amines [17]. The peaks due to the aromatic protons appeared as multiplet in the range $7.42\text{--}7.32\text{ ppm}$.

Figure 1b presents the ^{13}C -NMR spectrum of the complex. In the spectrum, the signal due to the methyl carbon was observed at 45.70 ppm , and the apparent highly deshielded position was due to the electronegative nitrogen. The $\text{N}13\text{CS}_2$ carbon signals resonated at 205 ppm . This peak position was within the region expected for metal dithiocarbamate complexes from the main group [16], which are often found around 200 ppm . It signified the contribution of a double-bond character to N-C bond, which was formally a single bond in the dithiocarbamate [18]. The aromatic carbon peaks resonated in the $147.40\text{--}125.40\text{ ppm}$ range.

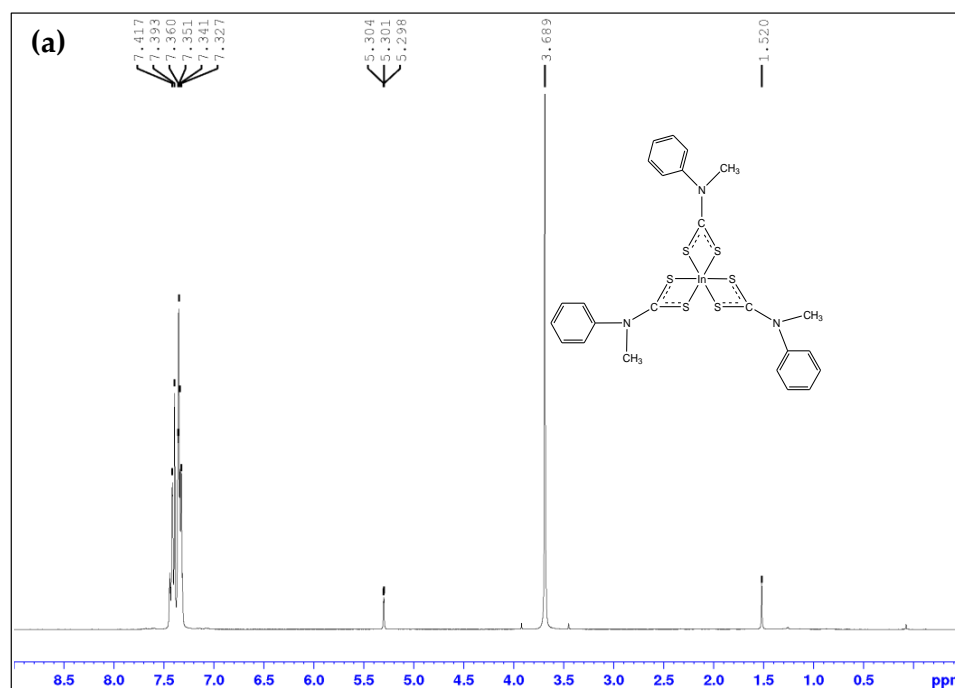


Figure 1. Cont.

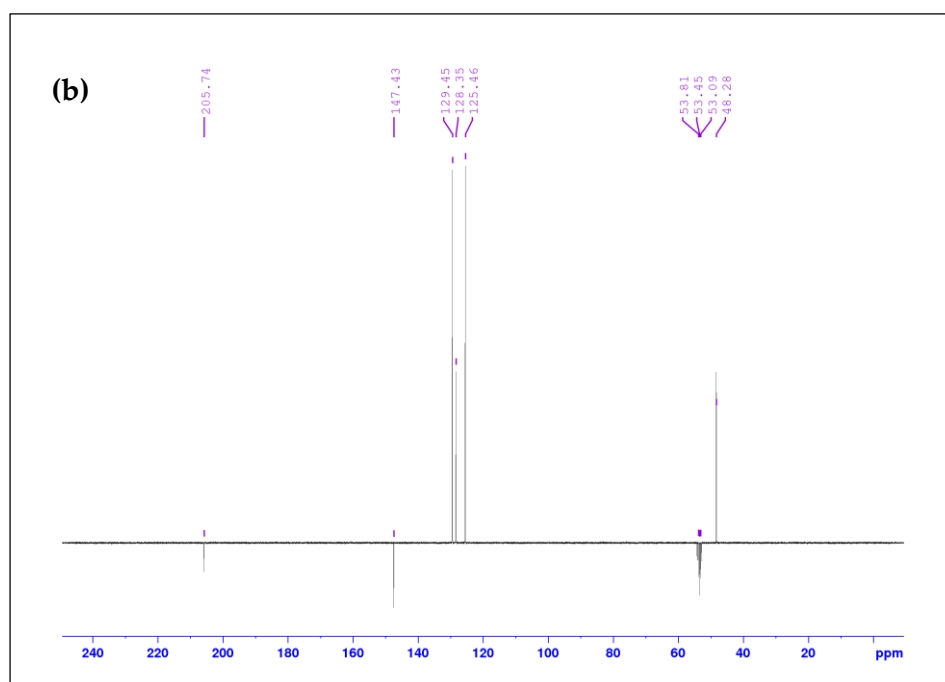


Figure 1. (a) ^1H and (b) ^{13}C NMR spectra of In(III) tris (*N*-methyl-*N*-phenyl dithiocarbamate).

2.2. Crystal Structure Description

Table 1 comprises the details of data collection and crystallographic parameters, while equivalent isotropic displacement parameters and atomic coordinates are presented in Table S1 (Supporting Information, SI). Table S2 in the SI provides some selected interatomic distances and bond angles.

Figure 2 presents a molecular drawing of the complex, which presents one of the molecules in the asymmetric unit. In the asymmetric unit of the complex, two symmetry-independent molecules are available, consisting of two In(III) tris (*N*-methyl-*N*-phenyldithiocarbamate) molecules. The indium is in the +3-oxidation state, and the balancing of the charge emanates from the three dithiocarbamate molecules in which there is a spreading of the negative charge over both S atoms. The two molecules in the asymmetric unit are related through pseudo-inversion in symmetry position $0.5-x, 1.5-y, 0.5-z$ for all atoms except for the bulky organic portion. The dithiocarbamate ligand uses both sulphur atoms to coordinate to the indium atom. Six sulphur atoms from three chelating dithiocarbamate moieties are arranged in a slightly disordered octahedral geometry around the In(III) atom in each molecule, with angles S-In-S varying from about $69.67(4)^\circ$ to $159.50(4)^\circ$ (In-S distances in the $2.5561(14)$ – $2.6352(13)$ Å range) (Table S2). The overall geometry of this complex is comparable to those determined for complexes related to dithiocarbamates [19–21]. All six In-S distances are similar and match well with the values in other previous reported studies [22,23]. Within experimental error, the C-S distances in the two molecules are comparable (close to 1.72 Å), which indicated a delocalization in the CS_2 skeleton. The C-N distances, which are close to 1.33 Å, are considerably shorter compared to a normal single bond. This is an indication that the metal dithiocarbamates have a significant double bond character. The four-membered ‘ MS_2C ’ rings are planar. The supramolecular arrangement of the complex shows the packing of molecules along the *c* axis forming layers parallel to the *b* axis (Figure 3). The crystal structure is stabilized by several non-covalent contacts such as weak hydrogen-bonding interactions and $\text{C-H}\cdots\text{S}$ and $\text{C-H}\cdots\pi$ interactions. The intermolecular interaction parameters are recapped in Tables 2 and 3.

Table 1. Crystallographic data for $[\text{InL}^1_3]$.

Complex	Indium(III) Tris (<i>N</i> -Methyl- <i>N</i> -phenyldithiocarbamate)
Empirical formula	$\text{C}_{24}\text{H}_{24}\text{InN}_3\text{S}_6$
Formula weight (g/mol)	661.64
Crystal system, space group	Triclinic, P-1
a (Å)	14.6017 (18)
b (Å)	14.9653 (18)
c (Å)	15.3953 (18)
α (°)	62.209 (2)
β (°)	76.315 (2)
γ (°)	72.310 (2)
V (Å ³)	2817.4 (6)
Z	4
μ (mm ⁻¹)	1.30
D_x (Mg m ⁻³)	1.560
$F(000)$	1336
Crystal size (mm)	0.20 × 0.16 × 0.13
Crystal habit	Block, colourless
$\theta_{\text{min}}/\theta_{\text{max}}$ (deg)	2.4/25.5
Observed refl. with $I > 2\sigma(I)$	8571
Measured reflections	57,388
Independent reflections	10,615
R_{int}	0.069
Data/restraints/parameters	10,615/0/607
wR(F^2)	0.160
$R[F^2 > 2\sigma(F^2)]$	0.053
Goof = S	1.11
$\Delta\rho_{\text{max}}/\Delta\rho_{\text{min}}$ (e.Å ⁻³)	3.22/−0.70
CCDC number	2184738

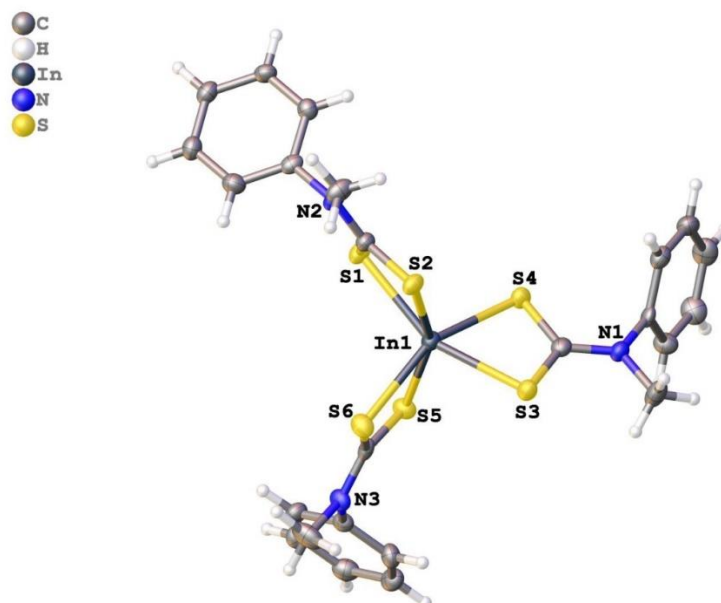


Figure 2. A molecular drawing of In(III) tris (*N*-methyl-*N*-phenyldithiocarbamate) presented with 50% probability ellipsoids. One of the molecules is shown in the asymmetric unit.

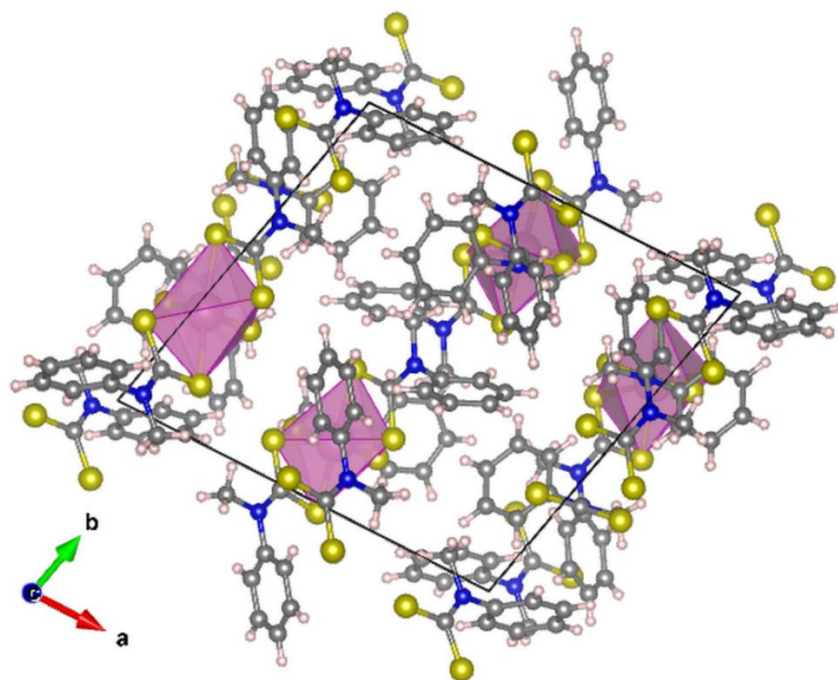


Figure 3. Crystal packing of In(III) tris (*N*-methyl-*N*-phenyldithiocarbamate) viewed along the *c*-axis showing the distorted octahedral coordinating polyhedrons.

Table 2. Short C-H...S hydrogen bonds (Å, °) in In(III) tris (*N*-methyl-*N*-phenyldithiocarbamate).

D-H...A	D-H	H...A	D...A	D-H...A
C17-H17...S10 ^{viii}	0.95	2.87	3.596(6)	135
C46-H46...S5 ^{vi}	0.95	2.97	3.521(6)	134

Symmetry codes: (vi) 1-*x*, 1-*y*, 1-*z*; (viii) *x*, 1 + *y*, -1 + *z*.

Table 3. Intermolecular C-H... π interactions (Å, °) in In(III) tris (*N*-methyl-*N*-phenyldithiocarbamate).

X-H...Cg	H...Cg	X...Cg	X-H...Cg
C(14)-H(14)...Cg(5)	2.58	3.517(7)	170
C(24)-H(24)...Cg(6)	2.54	3.472(6)	168
C(26)-H(26)...Cg(4)	2.64	3.580(6)	173
C(32)-H(32)...Cg(11)	2.53	3.464(7)	167
C(39)-H(39)...Cg(4)	2.82	3.516(7)	131
C(42)-H(42)...Cg(12)	2.58	3.486(7)	160
C(44)-H(44)...Cg(10)	2.51	3.392(6)	155

Symmetry codes: (i) -*x*, 1-*y*, -*z*; (ii) -*x*, 1-*y*, 1-*z*; (iii) -*x*, 2-*y*, -*z*; (iv) 1-*x*, -*y*, 1-*z*; (v) 1-*x*, 1-*y*, -*z*; (vi) 1-*x*, 1-*y*, 1-*z*; (vii) 1-*x*, -*y*, 2-*z*.

2.3. Hirshfeld Surface Analysis and 2D Fingerprints

To obtain qualitative and quantitative understandings into the complex's diverse intermolecular interactions, molecular Hirshfeld surfaces and the equivalent two-dimensional (2D) fingerprint plots were calculated [24,25]. Based on the single-crystal structure data, CrystalExplorer17.5 was used to create the Hirshfeld surfaces and 2D fingerprint plots [26]. Hirshfeld surfaces with different properties, such as d_e , d_{norm} , shape index, and curvedness, have been shown to be a useful visualization tool for analysing intermolecular interactions and molecule crystal packing behaviour [27,28]. The surfaces plotted over d_{norm} , shape index, and curvedness are shown in Figure 4. The 2D fingerprint plots of the complex are shown in Figure 5. The d_{norm} surface was mapped on a fixed colour scale ranging from -1.129 to 1.462. The Hirshfeld surface (HS) plotted with the complex's

d_{norm} value shows the zone formed with different colours, with red regions representing near contacts formed, white regions corresponding to weak interactions, and blue regions indicating the absence of important contacts. In the image, the red areas are spotlighted because the sum of the vdW radii is higher than the distance between the adjacent atoms. The dark-red spots on the complex's HS match the remarkable hydrogen-bonding contacts associated with the C-H \cdots S hydrogen bonds, as shown in Figure 4a. The other red cycles around the phenyl rings, to a lesser extent, characterize weak C \cdots H and C \cdots C interactions, i.e., C-H \cdots π and $\pi\cdots\pi$ surface interactions that play significant roles in supramolecular packing. Supplementary pairs of triangles are observable on the surfaces of both molecules for the shape index surface (Figure 4b) and indicate that the corresponding π -stacking interactions are available in the complex's crystal arrangement. Figure 4c presents the complex interactions, which correspond to the comparatively small regions of green flatness on the curved surfaces and are observable on both sides of the switched molecule.

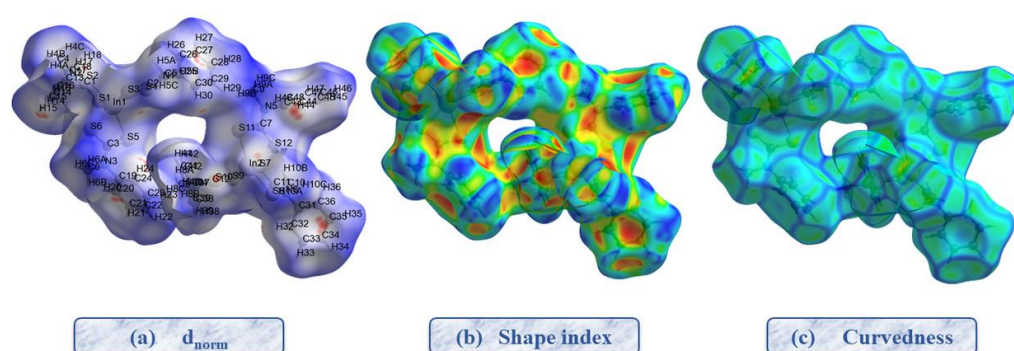


Figure 4. Hirshfeld surfaces (a) d_{norm} , (b) shape index, and (c) curvedness for In(III) tris (*N*-methyl-*N*-phenyldithiocarbamate) complex.

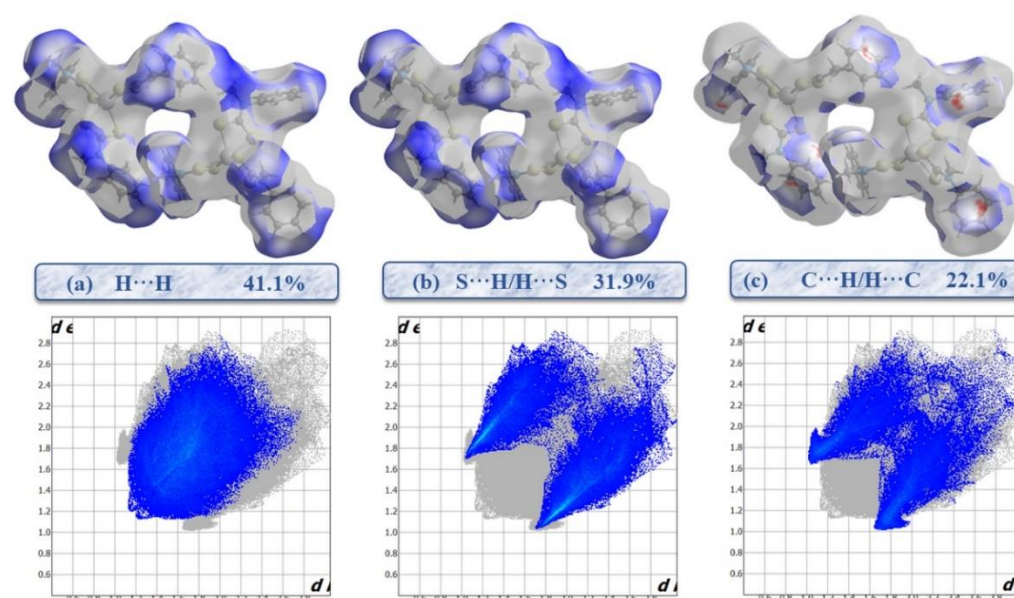


Figure 5. Two-dimensional fingerprint plots and their relative Hirshfeld surfaces as well as the contributions of the major interactions in the In(III) tris (*N*-methyl-*N*-phenyldithiocarbamate) complex.

Figure 5 depicts the overlay of major different contacts over the complex's HS. In the figure, the distinct blue colour region and spike length indicate the power of contacts that exist in the crystal packing. Usually, it is spoiled into a single contact that is of the type atom1 \cdots atom2 in order to illustrate the individual interaction types that are available. In Figure 5a, the H \cdots H interactions are found in the middle of the dispersed points in the FP and have a contribution of 41.1%, which is a large percentage, over the total HS, because

there is a coverage of the surface by a great number of H atoms. The S...H contact, including C-H...S intermolecular contacts, is shown as two pointed spikes in the FPs (Figure 5b). These interactions account for 31.7% and improve the crystal packing even more, as they account for the second largest contribution to total HS. As shown by the 'wings' which appear in the upper left as well as the lower right of the FP in Figure 5c, many H atoms reinforced the C-H... π contacts, making it the third important contribution with 22.67% of the total HS. Figure 6 shows the presence of additional contacts, including S...S, S...C, C...C, N...H, and N...C interactions, which account for 1.7%, 1.5%, 0.6%, 0.2% and 0.1% of all contacts that contribute to crystal packing.

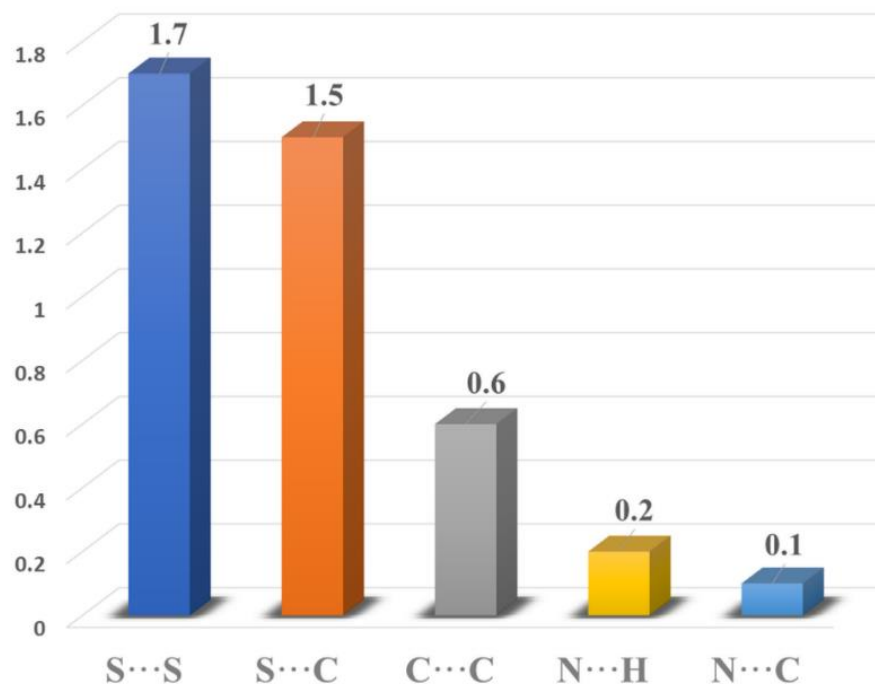


Figure 6. Distribution of the remaining intermolecular contacts based on the Hirshfeld surface analysis.

2.4. Thermal Studies

Figure 7 presents the TGA and DTA graphs of the complex. The TGA displayed only one decomposition peak, which occurred after the melting of the compounds. Stability was maintained up to 290 °C after which the decomposition of the complex commenced with melting. Subsequently, decomposition of the compounds in the temperature range 290–345 °C with about 70% weight loss occurred. The final residue corresponded to In_2S_3 , similar to previous reports on the thermal decomposition of In(III) tris (alkyldithiocarbamate) [13,29]. The DTA graph showed two endothermic peaks. The first DTA peak, which occurred around 297 °C, is ascribed to the melting point temperature, while the main DTA peak corresponds to the thermal breakdown of the dithiocarbamate complex, thereby leading to indium sulphide. The thermal decomposition of dithiocarbamate complexes could either proceed via the isothiocyanate intermediate or decompose directly in a one-step process to its metal sulphide. However, complexes may volatilize to leave behind a negligible amount of residue, and this has resulted to the categorisation of dithiocarbamate complexes as volatile or non-volatile complexes [30].

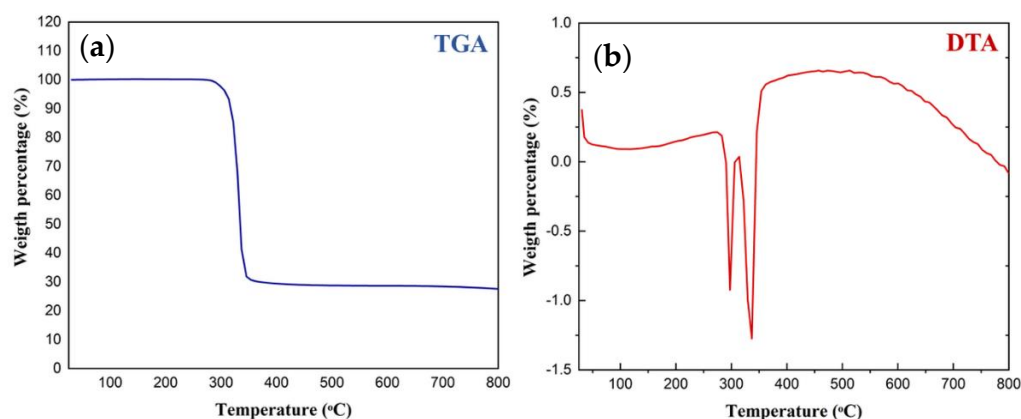


Figure 7. (a) TG and (b) DTA curves of indium(III) tris (*N*-methyl-*N*-phenyldithiocarbamate).

3. Materials and Methods

All the solvents and reagents employed were commercially available as analytical grade materials. They were used as received without any purification. The ligand, ammonium *N*-methyl-*N*-phenyl dithiocarbamate was prepared following a method reported previously [31]. Elemental analyses (C, H, N, S) was conducted on a HEKAtech CHNS Euro EA 3000 elemental analyser. Melting points measurement was obtained with open capillary tubes on a HWS MAINZ Laboratoriumstechnik SG 2000. ^1H and ^{13}C NMR spectra were measured in CDCl_3 solution on a Bruker Advance II 300 spectrometer. The FTIR spectrum was recorded in the frequency range $4000\text{--}400\text{ cm}^{-1}$ on a Bruker IFS 66 v/S. Thermogravimetric analysis (TGA) was carried out on TGA/DSC1 (Mettler-Toledo GmbH, Gießen, Germany) instrument, with a simultaneous TG and DTA measurement facility. The thermogravimetric curve was recorded under nitrogen flow at a heating rate of $5\text{ }^\circ\text{C}/\text{min}$, and a plot of mass loss of sample as a function of temp. gradient was recorded.

3.1. Preparation of Tris (*N*-Methyl-*N*-phenyldithiocarbamate) Indium(III)

A 15 mL aqueous solution of indium(III) sulphate (1.0 mmol) was reacted with 10 mL aqueous solution of ammonium *N*-methyl-*N*-phenyldithiocarbamate (3.0 mmol) for 1 h. The resultant precipitates were filtered and rinsed with water/ethanol solution (1:1). Single crystal suitable for analysis was obtained in a solution of dichloromethane/ethanol (3:1).

Yield: 81%, M.p. $296\text{ }^\circ\text{C}$. ^1H NMR (CD_2Cl_2) $\delta = 7.42\text{--}7.32$ (m, 10H, $-\text{C}_6\text{H}_5$), 3.69 (s, 6H, $-\text{N-CH}_3$). ^{13}C NMR (CDCl_3) δ 147.43, 129.45, 128.35, 125.46 ($-\text{C}_6\text{H}_5$), 48.28 ($-\text{CH}_3$), 205.74 ($-\text{CS}_2$). Selected FTIR, ν (cm^{-1}): 1492 (C=N), 1382 ($\text{C}_2\text{-N}$), 977 (C=S), 3049 (=CH), 2978 ($-\text{CH}$). Anal. Calc. for $\text{C}_{24}\text{H}_{24}\text{N}_3\text{S}_6\text{In}$ (661.67): C, 43.57; H, 3.66; N, 6.35; S, 29.08. Found: C, 43.61; H, 3.57; N, 6.34; S, 29.23.

3.2. Single-Crystal X-ray Measurements

X-ray data of a clear, colourless crystal with estimated dimensions of $0.134 \times 0.158 \times 0.195\text{ mm}^3$ were collected at $100(2)\text{ K}$ on a Bruker APEXII CCD DUO diffractometer with $\text{Mo K}\alpha$ ($\lambda = 0.71073\text{ \AA}$) radiation [32]. Data reduction was achieved using SAINT [32]. A direct method with SHELXS which uses the SHELXTL package was used to solve the structure. A full-matrix least squares procedures was used to refine the structure on F^2 with the program SHELXL-2015 [33,34]. All non-hydrogen atoms were refined using anisotropic displacement parameters, and the hydrogen atoms were placed at calculated positions using a riding model. The final difference Fourier map had a significant proportion of residual electron density that could not be modelled, and this was attributed to residual electron density from the heavily absorbing Indium atom in the structure. Olex2 was used to prepare molecular graphics of the compound [35] and Vesta software [36].

4. Conclusions

In this study, we have synthesized and characterized a novel In(III) tris (*N*-methyl-*N*-phenyldithiocarbamate) complex. It comprises two symmetry-independent In(III) tris (*N*-methyl-*N*-phenyldithiocarbamate) molecules. The Indium atom shows a hexa-coordinate geometry by virtue of the chelation of three dithiocarbamate ligands. The packing arrangement was mainly stabilized by C-H \cdots S hydrogen bonding networks and C-H \cdots π interactions. Hirshfeld surface analysis shows that H \cdots H interactions accounted for 41.1% of the complex's total Hirshfeld surface. Spectroscopic studies corroborated the structural analysis, which confirmed that the complex was formed through the symmetric coordination of the sulphur atoms to the indium atom. Evaluation of the thermal stability of the complex showed that it is stable up to 290, after which decomposition proceeds up to 345 °C with about 70% weight loss to give the metal sulphide. The thermal studies conformed the suitability of the complex as a good single source precursor for the formation of indium sulphide nanoparticles, which might find applications in opto-electronic devices.

Supplementary Materials: The following supporting information can be downloaded at: <https://www.mdpi.com/article/10.3390/inorganics10100146/s1>, Table S1: Equivalent isotropic displacement parameters and atomic coordinates; Table S2: Some selected interatomic distances and bond angles.

Author Contributions: Conceptualization, D.C.O. and H.F.; methodology, D.C.O. and H.F.; software, D.C.O. and H.F.; validation, D.C.O. and H.F.; formal analysis, D.C.O. and H.F.; investigation, D.C.O. and H.F.; resources, D.C.O. and H.F.; data curation, D.C.O. and H.F.; writing—original draft preparation, D.C.O. and H.F.; writing—review and editing, D.C.O. and H.F.; visualization, D.C.O. and H.F.; supervision, D.C.O.; project administration, D.C.O. and H.F.; funding acquisition, H.F. All authors have read and agreed to the published version of the manuscript.

Funding: This research was funded by the Deanship of Scientific Research at Imam Mohammad Ibn Saud Islamic University grant number RG-21-09-68.

Data Availability Statement: Not applicable.

Acknowledgments: The authors extend their appreciation to the Deanship of Scientific Research at Imam Mohammad Ibn Saud Islamic University for funding this work through Research Group no. RG-21-09-68.

Conflicts of Interest: The authors declare no conflict of interest.

References

1. Raṭ, C.I.; Silvestru, C.; Breunig, H.J. Hypervalent organoantimony and-bismuth compounds with pendant arm ligands. *Coord. Chem. Rev.* **2013**, *257*, 818–879. [CrossRef]
2. Braunschweig, H.; Cogswell, P.; Schwab, K. Synthesis, structure and reactivity of complexes containing a transition metal–bismuth bond. *Coord. Chem. Rev.* **2011**, *255*, 101–117. [CrossRef]
3. Scozzafava, A.; Mastrolorenzo, A.; Supuran, C.T. Arylsulfonyl-*N,N*-diethyl-dithiocarbamates: A novel class of antitumor agents. *Bioorg. Med. Chem. Lett.* **2000**, *10*, 1887–1891. [CrossRef]
4. Matesanz, A.I.; Pérez, J.M.; Navarro, P.; Moreno, J.M.; Colacio, E.; Souza, P. Synthesis and characterization of novel palladium (II) complexes of bis (thiosemicarbazone). Structure, cytotoxic activity, and DNA binding of Pd (II)-benzyl bis (thiosemicarbazone). *J. Inorg. Biochem.* **1999**, *76*, 29–37. [CrossRef]
5. Ferreira, I.; De Lima, G.; Paniago, E.; Takahashi, J.; Pinheiro, C. Synthesis, characterization, and antifungal activity of new dithiocarbamate-based complexes of Ni (II), Pd (II) and Pt (II). *Inorg. Chim. Acta* **2014**, *423*, 443–449. [CrossRef]
6. Nieuwenhuizen, P.J. Zinc accelerator complexes: Versatile homogeneous catalysts in sulfur vulcanization. *Appl. Catal. A Gen.* **2001**, *207*, 55–68. [CrossRef]
7. Wang, Z.-Q.; Lu, S.-W.; Guo, H.-F.; Hu, N.-H. Synthesis, properties, and molecular structure of five-coordinate N, N-dibenzyl dithiocarbamate complexes of titanocene, zirconocene and hafnocene. *Polyhedron* **1992**, *11*, 1131–1135. [CrossRef]
8. Grainger, R.S.; Innocenti, P. New applications of dithiocarbamates in organic synthesis. *Heteroat. Chem. Int. J. Main Group Elem.* **2007**, *18*, 568–571.
9. Ozturk, I.; Banti, C.N.; Kourkoumelis, N.; Manos, M.J.; Tasiopoulos, A.J.; Owczarzak, A.; Kubicki, M.; Hadjikakou, S.K. Synthesis, characterization and biological activity of antimony (III) or bismuth (III) chloride complexes with dithiocarbamate ligands derived from thiuram degradation. *Polyhedron* **2014**, *67*, 89–103. [CrossRef]

10. Garje, S.S.; Jain, V.K. Chemistry of arsenic, antimony and bismuth compounds derived from xanthate, dithiocarbamate and phosphorus-based ligands. *Coord. Chem. Rev.* **2003**, *236*, 35–56. [[CrossRef](#)]
11. Chaudhari, K.R.; Yadav, N.; Wadawale, A.; Jain, V.K.; Bohra, R. Monoorganobismuth (III) dithiocarboxylates: Synthesis, structures and their utility as molecular precursors for the preparation of Bi₂S₃ films and nanocrystals. *Inorg. Chim. Acta* **2010**, *363*, 375–380. [[CrossRef](#)]
12. Sivasekar, S.; Ramalingam, K.; Rizzoli, C. Metal dithiocarbamate precursors for the preparation of a binary sulfide and a pyrochlore: Synthesis, structure, continuous shape measure and bond valence sum analysis of antimony (III) dithiocarbamates. *Polyhedron* **2015**, *85*, 598–606. [[CrossRef](#)]
13. Dutta, D.P.; Jain, V.; Chaudhury, S.; Tiekink, E. Indium tris N-methylpiperazinylcarbodithioate: Synthesis, structure and its transformation into indium sulfide. *Main Group Met. Chem.* **2001**, *24*, 405–408. [[CrossRef](#)]
14. Ronconi, L.; Giovagnini, L.; Marzano, C.; Bettio, F.; Graziani, R.; Pilloni, G.; Fregona, D. Gold dithiocarbamate derivatives as potential antineoplastic agents: Design, spectroscopic properties, and in vitro antitumor activity. *Inorg. Chim. Acta* **2005**, *44*, 1867–1881. [[CrossRef](#)]
15. Gurumoorthy, G.; Rani, P.J.; Thirumaran, S.; Ciattini, S. Cobalt (III) dithiocarbamates for anion sensing and preparation of cobalt sulfide and cobalt-iron sulfide nanoparticles: Photocatalytic degradation of dyes with as-prepared nanoparticles. *Inorg. Chim. Acta* **2017**, *455*, 132–139. [[CrossRef](#)]
16. Tamilvanan, S.; Gurumoorthy, G.; Thirumaran, S.; Ciattini, S. Synthesis, characterization, cytotoxicity and antimicrobial studies on Bi (III) dithiocarbamate complexes containing furfuryl group and their use for the preparation of Bi₂O₃ nanoparticles. *Polyhedron* **2017**, *121*, 70–79. [[CrossRef](#)]
17. Bonati, F.; Ugo, R. Organotin (iv) n, n-disubstituted dithiocarbamates. *J. Organomet. Chem.* **1967**, *10*, 257–268. [[CrossRef](#)]
18. Van Gaal, H.; Diesveld, J.; Pijpers, F.; Van der Linden, J. Carbon-13 NMR spectra of dithiocarbamates. Chemical shifts, carbon-nitrogen stretching vibration frequencies and pi-bonding in the NCS₂ fragment. *Inorg. Chim. Acta* **1979**, *18*, 3251–3260. [[CrossRef](#)]
19. Tan, Y.S.; Yeo, C.I.; Tiekink, E.R.; Heard, P.J. Dithiocarbamate complexes of platinum group metals: Structural aspects and applications. *Inorganics* **2021**, *9*, 60. [[CrossRef](#)]
20. Gowda, V.; Sarma, B.; Larsson, A.C.; Lantto, P.; Antzutkin, O.N. Bi (III) Complexes Containing Dithiocarbamate Ligands: Synthesis, Structure Elucidation by X-ray Diffraction, Solid-State ¹³C/¹⁵N NMR, and DFT Calculations. *ChemistrySelect* **2020**, *5*, 8882–8891. [[CrossRef](#)]
21. Dutta, D.P.; Jain, V.K.; Knoedler, A.; Kaim, W. Dithiocarbamates of gallium (III) and indium (III): Syntheses, spectroscopy, and structures. *Polyhedron* **2002**, *21*, 239–246. [[CrossRef](#)]
22. Jain, V.K.; Wadawale, A.; Kushwah, N.P.; Pal, M.K. Organo-gallium and indium complexes with dithiolate and oxo ligands: Synthesis, structures and applications. *J. Chem. Sci.* **2011**, *123*, 107–112. [[CrossRef](#)]
23. Saiyed, T.A.; Adeyemi, J.O.; Onwudiwe, D.C. The structural chemistry of zinc (ii) and nickel (ii) dithiocarbamate complexes. *Open Chem.* **2021**, *19*, 974–986. [[CrossRef](#)]
24. Spackman, M.A.; Jayatilaka, D. Hirshfeld surface analysis. *CrystEngComm* **2009**, *11*, 19–32. [[CrossRef](#)]
25. Spackman, M.A.; McKinnon, J.J. Fingerprinting intermolecular interactions in molecular crystals. *CrystEngComm* **2002**, *4*, 378–392. [[CrossRef](#)]
26. Spackman, P.R.; Turner, M.J.; McKinnon, J.J.; Wolff, S.K.; Grimwood, D.J.; Jayatilaka, D.; Spackman, M.A. CrystalExplorer: A program for Hirshfeld surface analysis, visualization and quantitative analysis of molecular crystals. *J. Appl. Crystallogr.* **2021**, *54*, 1006–1011. [[CrossRef](#)]
27. Ferjani, H.; Ben Smida, Y.; Onwudiwe, D.C.; Elamin, N.Y.; Ezzine, S.; Almotlaq, N.S. An Experimental and Theoretical Study of the Optical Properties of (C₂H₇N₄O)₂BiCl₅ for an Optoelectronic Application. *Inorganics* **2022**, *10*, 48. [[CrossRef](#)]
28. Setifi, Z.; Ferjani, H.; Jelsch, C.; Glidewell, C.; Dege, N.; Setifi, F. Synthesis, Structure and Hirshfeld Surface Analysis of a New Iron Complex [Fe(N₄Py)(tcnspr)](tcnspr). *J. Inorg. Organomet. Polym. Mater.* **2021**, *31*, 3054–3061. [[CrossRef](#)]
29. Bessergenev, V.G.; Bessergenev, A.V.; Ivanova, E.N.; Kovalevskaya, Y.A. Study of In₂S₃ Thin Films by Diffraction of Synchrotron Radiation. *J. Solid-State Chem.* **1998**, *137*, 6–11. [[CrossRef](#)]
30. Bajpai, A.; Tiwari, S. Application of thermogravimetric analysis for characterisation of bisdithiocarbamate of urea and its copper (II) complex. *Thermochim. Acta* **2004**, *411*, 139–148. [[CrossRef](#)]
31. Onwudiwe, D.C.; Ajibade, P.A. Synthesis and characterization of metal complexes of N-alkyl-N-phenyl dithiocarbamates. *Polyhedron* **2010**, *29*, 1431–1436. [[CrossRef](#)]
32. Bruker AXS Inc. *APEX2, Version 2014.11-0*; Bruker AXS Inc.: Madison, WI, USA, 2014.
33. Sheldrick, G.M. SHELXT-Integrated space-group and crystal-structure determination. *Acta Crystallogr. Sect. A Found. Adv.* **2015**, *71*, 3–8. [[CrossRef](#)] [[PubMed](#)]
34. Sheldrick, G.M. Crystal structure refinement with SHELXL. *Acta Crystallogr. Sect. C Struct. Chem.* **2015**, *71*, 3–8. [[CrossRef](#)] [[PubMed](#)]
35. Dolomanov, O.; Bourhis, L.; Gildea, R.; Howard, J.; Puschmann, H. OLEX2: A Complete Structure Solution, Refinement and Analysis Program. *J. Appl. Crystallogr.* **2009**, *42*, 339–341. [[CrossRef](#)]
36. Momma, K.; Izumi, F. VESTA 3 for three-dimensional visualization of crystal, volumetric and morphology data. *J. Appl. Crystallogr.* **2011**, *44*, 1272–1276. [[CrossRef](#)]